Determining what global warming of 1.5°C and higher means for the semi-arid regions of Botswana, Namibia, Ghana, Mali, Kenya and Ethiopia:

A description of ASSAR's methods of analysis

CARIAA
Collaborative Adaptation Research Initiative in Africa and Asia

ASSAR
Adaptation at Scale in Semi-Arid Regions

About ASSAR Working Papers

This series is based on work funded by Canada's International Development Research Centre (IDRC) and the UK's Department for International Development (DFID) through the Collaborative Adaptation Research Initiative in Africa and Asia (CARIAA). CARIAA aims to build the resilience of vulnerable populations and their livelihoods in three climate change hot spots in Africa and Asia. The program supports collaborative research to inform adaptation policy and practice.

Titles in this series are intended to share initial findings and lessons from research and background studies commissioned by the program. Papers are intended to foster exchange and dialogue within science and policy circles concerned with climate change adaptation in vulnerability hotspots. As an interim output of the CARIAA program, they have not undergone an external review process. Opinions stated are those of the author(s) and do not necessarily reflect the policies or opinions of IDRC, DFID, or partners. Feedback is welcomed as a means to strengthen these works: some may later be revised for peer-reviewed publication.

Contact

Collaborative Adaptation Research Initiative in Africa and Asia
c/o International Development Research Centre
PO Box 8500, Ottawa, ON
Canada K1G 3H9
Tel: (+1) 613-236-6163; Email: cariaa@idrc.ca

Funded by:

UKaid from the British people

IDRC | CRDI
International Development Research Centre
Centre de recherches pour le développement international

Canada

Determining what global warming of 1.5°C and higher means for the semi-arid regions of Botswana, Namibia, Ghana, Mali, Kenya and Ethiopia:

A description of ASSAR's methods of analysis

Contributing authors:

Tiro Nkemelang[1]

Roy Bouwer[1]

Tali Hoffman[1]

Mark New[1]

[1]University of Cape Town (UCT)

Private Bag X3

Rondebosch

7701

South Africa

http://www.uct.ac.za/

Table of Contents

List of Figures

List of Tables

1. Background

Developing nations are the most vulnerable to the impacts of climate change. This is particularly true for semi-arid regions (SAR) – climate change hotspots characterised by limited resources, remoteness, susceptibility to natural disasters, vulnerability to external shocks, and fragile environments. In these hotspots, an increase of just half a degree in global temperatures might have a significant effect, as seemingly-small temperature increments can lead to distinct climatological conditions at the local level.

In October 2018, the International Panel on Climate Change (IPCC) released a special report on the impacts of global warming of 1.5°C (IPCC, 2018) above pre-industrial levels – the target set by the Paris Agreement in 2015. To coincide with this IPCC report, ASSAR developed a set of country-specific analyses that examine how projected 1.5°C and higher (half degree increments up to 3°C) global warming could affect temperatures, precipitation, and climate extremes within the semi-arid and arid regions of each of the African countries where ASSAR works, namely: Botswana, Ethiopia, Ghana, Kenya, Mali, and Namibia. We also explore how these local-level climate changes would impact on water, agriculture, health and other vulnerable sectors in these areas.

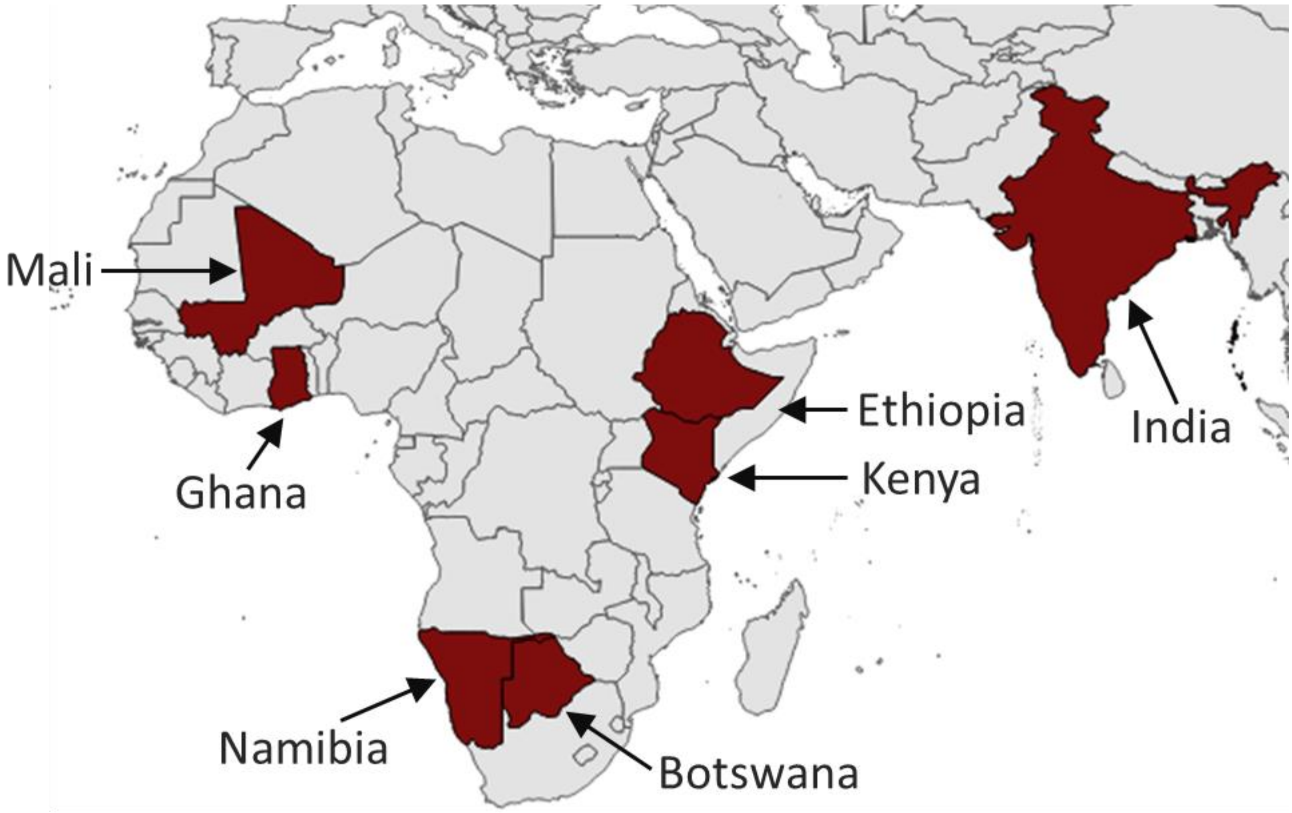

Figure 1: Map of all ASSAR study countries.

The timing of this work is critical as global temperatures could exceed the 1.5°C threshold by as early as 2026 (Henley and King, 2017). Other estimates indicate that in the absence of considerable emission reductions the world will cross the 1.5°C threshold around 2040. All estimates suggest an urgent need to accelerate local-level adaptation responses.

2. Data analysis

a) Calculating aridity zones

We used the Global Aridity Index (GAI; Trabucco and Zomer, in press) to divide ASSAR's African countries into distinct aridity zones (Table 1).

Table 1: Global Aridity Index (GAI) classification.

GAI VALUE	CLIMATE ZONE
<0.03	Hyper arid
0.03 – 0.2	Arid
0.2 – 0.5	Semi-arid
0.5 – 0.65	Dry sub-humid
> 0.65	Humid

The GAI is calculated using mean annual precipitation (MAP) and mean annual evapotranspiration (MAE) according to equation (1) below:

$$\text{GAI} = MAP/MAE \qquad (1)$$

We used MAP and MAE data from the high resolution (~30 arc seconds at equator) WorldClim Global Climate Dataset (Hijmans *et al.*, 2005), and used ArcGIS to create shapefiles of the different aridity zones for each ASSAR country. Due to the high spatial resolution of the GAI dataset, we removed smaller features by using QGIS to smooth the shapefiles. This smoothing did not have any significant impact on our results due to the low resolution the Global Climate Model (GCM) data used.

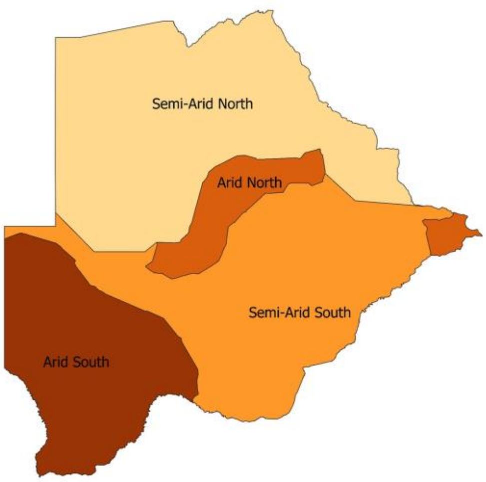

Botswana

According to the GAI classification, Botswana can be divided into two aridity zones, namely arid and semi-arid. The arid zone covers the south-western parts of the country, with an outcrop over central Botswana, while the semi-arid zone covers the bulk of eastern and northern Botswana. To distinguish between areas of homogeneous rainfall within the semi-arid zone, we further divided it into north and south sections following the homogeneous rainfall clustering used in Nkemelang *et al.* (2018).

Namibia

The GAI divides Namibia into three aridity zones: hyper-arid (coastal area bordering the Atlantic Ocean), arid (over central Namibia), and semi-arid (over the north-eastern parts of the country). The arid and semi-arid zones were further subdivided into north and south sections based on rainfall homogeneity using a similar method as for Botswana.

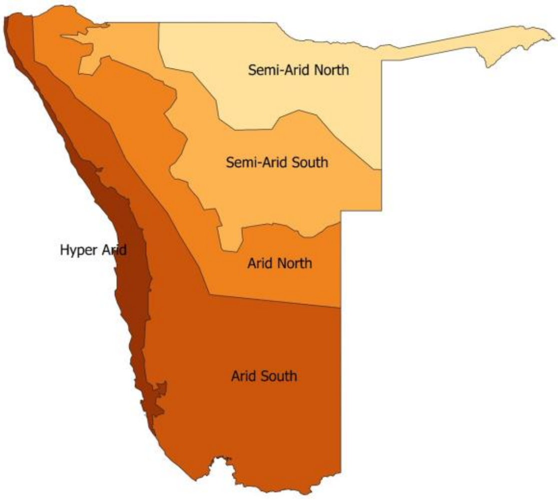

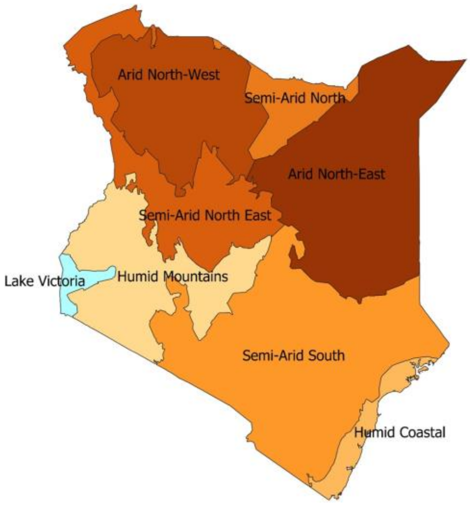

Kenya

The GAI divides Kenya into four aridity zones, namely arid, semi-arid, humid and dry sub-humid. We subdivided these further to take the geographical diversity in the weather and climate systems into account. We also merged the dry sub-humid zone with the humid zone as the former covered only a very small area.

Ethiopia

The GAI also divides Ethiopia into four aridity zones, namely arid, semi-arid, humid and dry sub-humid. As for Kenya, we further subdivided these to take the geographical diversity in the weather and climate systems into account, and merged the sub-humid zone with the humid zone.

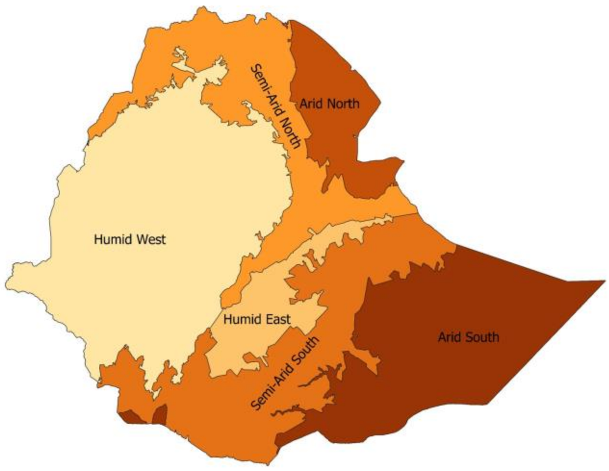

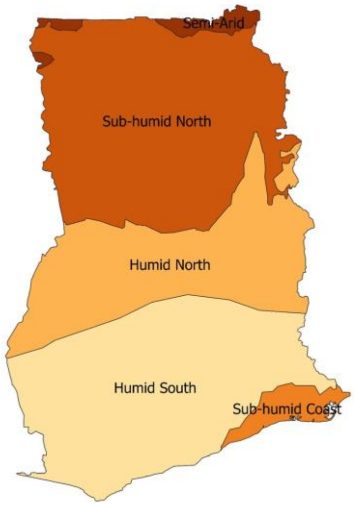

Ghana

Ghana is a predominantly humid country, classified by the GAI into semi-arid, dry sub-humid and humid zones. The semi-arid zone is confined to the north of the country and is relatively small. We subdivided the dry sub-humid zone into north and coastal sections, based on geography, and subdivided the humid zone into humid-north and humid-south following the agro-ecological zones defined by the Ghana Meteorological Agency (Amekudzi *et al.,* 2015).

Mali

The GAI divided Mali into five distinct aridity zones, with aridity increasing from south to north. As the humid zone in the southernmost part of Mali was very small, we merged it with the dry sub-humid zone. We did not subdivide the zones any further.

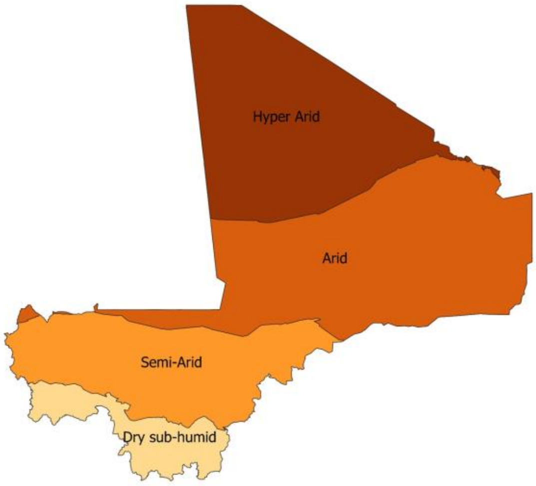

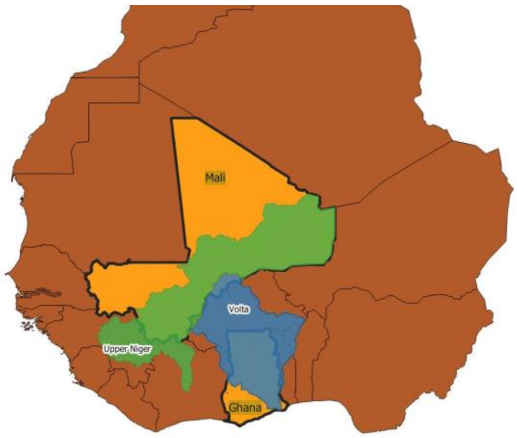

West Africa’s major river catchments

Two major river systems provide water for Ghana and Mali. In Ghana, we investigated changes in total annual precipitation over the Lake Volta catchment area. We extracted the shapefile for the catchment from the World Resources Institute major basins dataset (Food Agriculture Organization, 2006). For Mali, we considered the upstream section of the Niger River catchment that borders with Niger.

b) Mean climate and extreme indices

Following Nkemelang *et al.* (2018), we analysed mean annual surface temperature (TAS), and Expert Team on Climate Change Detection and Indices (ETCCDI) temperature and precipitation extreme indices, derived from models from the 5th version of the Coupled Model Intercomparison Project (CMIP5) program (Table 2). Following Taylor *et al.* (2012), we combined historical simulations (1861-2005) with a high emissions scenario (RCP8.5) and a midrange mitigation emissions scenario (RCP4.5). We downloaded 24 (RCP8.5) and 20 (RCP4.5) CMIP5 GCM outputs developed by Sillmann *et al.* (2013a) from the KNMI Climate Explorer database (Trouet and Van Oldenborgh, 2013) for each ETCCDI index (see Table 2). We included the RCP4.5 pathway in our analyses in order look for any significant differences in the relative changes at the respective warming levels, due to forcing differences – particularly aerosols. Where more than one model simulation was available, we chose the first ensemble member for analysis.

We focused on temperature and rainfall means for each ASSAR country, as well as indices of climatic extremes that directly relate to local climate change vulnerabilities (see Table 2 for details of each). We used TAS and total annual rainfall (PRCPTOT) to describe the mean climate. TAS helped us determine how the countries and their respective zones warm relative to global warming, and changes in PRCPTOT helped us determine possible annual rainfall deficits or surpluses that arise due to the warming climate. We used rainfall extreme indices (R99P, R95P, RX1DAY, RX5DAY, R20MM and R10MM) to relate the changes in heavy rainfall extremes, ALTCWD wet periods, and ALTCDD dry periods. We included an analysis of absolute extreme precipitation indices, even though climate models generally perform poorly in the representation of absolute rainfall (owing to limitations in how the models represent processes that drive precipitation extremes; Dai, 2006; Westra *et al.,* 2014). We did this because, despite the tendency of climate models to precipitate frequently due to the inherent limitations, they do manage to capture occurrences of precipitation extremes (O'Gorman, 2015). For temperature-derived indices, we used the warm spell duration index (WSDI) to determine the potential impact of heat waves (continuously high temperatures; Moses, 2017). We also included TN90P, TN10P, TX10P and TN10P to help determine the potential impact of discrete hot and cold events (Klein Tank *et al.,* 2009).

Table 2: Example (for Botswana) of country-specific extreme temperature and precipitation indices relevant to vulnerability assessments. The indices are available from the KNMI Climate Explorer website.

INDEX	DESCRIPTION	UNITS
	Precipitation Indices	
PRCPTOT	Annual total precipitation in wet days	mm/year
ALTCDD	Maximum number of consecutive days per year with <1mm of precipitation	days
ALTCWD	Maximum number of consecutive days per year with at least 1mm of precipitation	days
RX1DAY	Annual maximum 1-day precipitation	mm/day
RX5DAY	Annual maximum 5-day precipitation	mm/5day
R99P	Annual total precipitation when daily precipitation > 99th percentile of wet day precipitation	mm/year
R95P	Annual total precipitation when daily precipitation >95th percentile of wet day precipitation	mm/year
R20MM	Annual count of days with at least 20mm of precipitation	days
R10MM	Annual count of days with at least 10mm of precipitation	days
	Temperature indices	
TAS	Mean annual surface temperature	°C
TX90P	% of days when daily maximum temperature is >90th percentile	%
TN90P	% of days when daily minimum temperature is >90th percentile	%
TX10P	% of days when daily minimum temperature is <10th percentile	%
TN10P	% of days when daily minimum temperature is <10th percentile	%
WSDI	Maximum number of consecutive days per year when daily maximum temperature >90th percentile	days

c) Calculating climate projections

Following Nkemelang *et al.* (2018), we used a 40-year (1861-1900) base period for the pre-industrial era. We defined the years at which each participating model reached 1.0°C, 1.5°C and 2.0°C global warming above pre-industrial levels for RCP4.5, and the years at which the models reached 1.0°C, 1.5°C, 2.0°C, 2.5°C and 3.0°C global warming above pre-industrial levels for RCP8.5.

We extended our analyses to 2.5°C and 3.0°C global warming to investigate whether additional 0.5°C increments at higher warming thresholds would have any impact on the results. For the RCP4.5 pathway we limited the warming thresholds to 2.0°C warming above pre-industrial levels, as for most participating models in this pathway, warming is not sufficiently strong to reach 2.5°C and 3.0°C warming (IPCC, 2014). For each model ensemble member we applied a 31-year running mean to the entire time-series. The climatology at a given global warming level is defined by the year the running mean reaches that global warming level and then stays consistently above it. The years at which the participating ensemble members reached the global warming levels are outlined in Table 3 below. Figure 2 indicates the year at which 100% of the models agree that we will reach each global warming increment.

Table 3: List of models used, and the years at which the 31-year running means of the ensemble members reached 1.0°C, 1.5°C, 2.0°C, 2.5°C and 3.0°C warming above pre-industrial levels.

RCP 8.5						RCP 4.5			
	Warming (°C)					Warming (°C)			
MODEL	**1.0**	**1.5**	**2.0**	**2.5**	**3.0**	**MODEL**	**1.0**	**1.5**	**2**
ACCESS1-0	2011	2026	2038	2050	2060	ACCESS1-0	2009	2029	2050
bcc-csm1-1	1999	2021	2038	2050	2061	bcc-csm1-1	2000	2023	2046
CanESM2	2001	2014	2027	2038	2049	bcc-csm1-1-m	2001	2017	2047
CCSM4	1996	2013	2030	2045	2057	CanESM2	2002	2017	2032
CMCC-CM	2015	2030	2042	2052	2062	CCSM4	1996	2016	2040
CMCC-CMS	2016	2030	2041	2052	2061	CMCC-CM	2015	2035	2052
CNRM-CM5	2012	2031	2045	2057	2067	CMCC-CMS	2017	2035	2053
CSIRO-Mk3-6-0	2018	2033	2045	2055	2065	CNRM-CM5	2013	2037	2059
GFDL-CM3	2011	2022	2035	2045	2054	CSIRO-Mk3-6-0	2019	2035	2048
GFDL-ESM2G	2014	2037	2054	2068	2080	HadGEM2-CC	2021	2036	2053
GFDL-ESM2M	2012	2035	2052	2067	2081	HadGEM2-ES	2010	2027	2042
HadGEM2-CC	2016	2027	2039	2049	2057	IPSL-CM5A-LR	1995	2013	2031
HadGEM2-ES	2009	2021	2034	2045	2054	IPSL-CM5B-LR	2000	2025	2047
inmcm4	2022	2044	2058	2070	2084	MIROC5	2017	2040	2069
IPSL-CM5A-LR	1995	2011	2027	2038	2048	MIROC-ESM	2005	2020	2034
IPSL-CM5A-MR	2002	2017	2031	2042	2051	MIROC-ESM-CHEM	2010	2024	2038
IPSL-CM5B-LR	1999	2021	2036	2049	2061	MPI-ESM-LR	1999	2021	2044
MIROC5	2014	2033	2048	2061	2072	MPI-ESM-MR	2003	2027	2049
MIROC-ESM	2006	2020	2030	2041	2051	MRI-CGCM3	2026	2054	2084
MIROC-ESM-CHEM	2009	2021	2032	2042	2052	NorESM1-M	2020	2043	2078
MPI-ESM-LR	2000	2018	2035	2049	2061				
MPI-ESM-MR	2003	2023	2039	2051	2062				
MRI-CGCM3	2025	2040	2052	2064	2075				
NorESM1-M	2017	2035	2049	2062	2074				

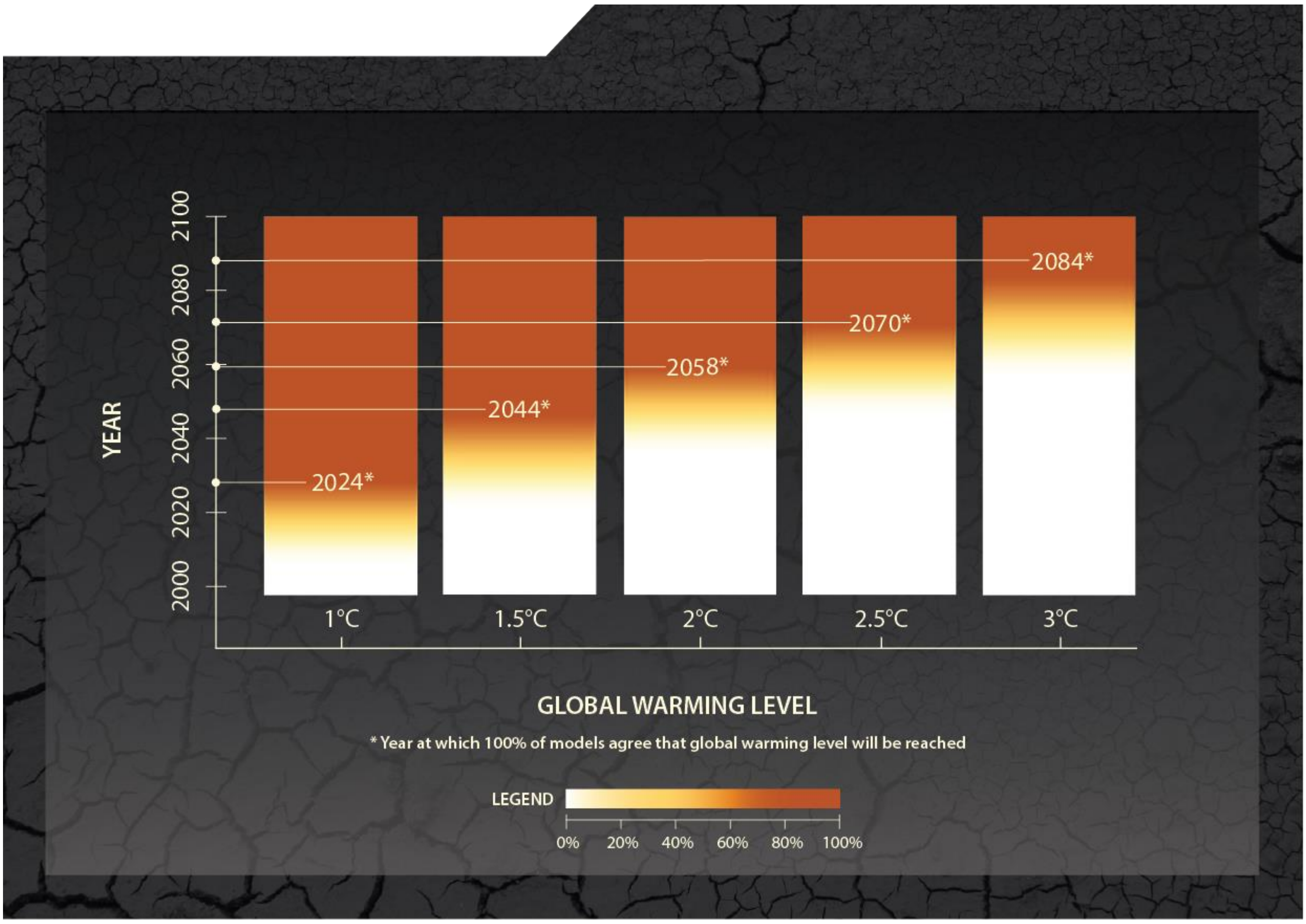

Figure 2: The years at which 100% of the models agree that each global warming increment will be reached.

For the indices within each subset, we calculated area-averaged climatological means at given global warming levels to determine the change relative to pre-industrial levels. For all the participating members, we calculated the change for each extreme index as:

$$\Delta I = I_n - I_0 \qquad (2)$$

where $I_n, n \in (1.0, 1.5, 2.0, 2.5\ and\ 3)$ for RCP8.5 and $I_n, n \in (1.0, 1.5\ and\ 2.0)$ for RCP4.5, represents the area-averaged climatological mean calculated from the 31-year period surrounding the date of global warming, and I_0 is the area-averaged climatological mean of the index of interest for 1861-1900 pre-industrial times. We plotted box-and-whisker plots (see Figure 3 for example) of the absolute changes for each climate extreme index spanning the ensemble for each zone and over the country area average.

Following previous studies (Kharin *et al.,* 2013; Sillmann *et al.,* 2013b), we used the non-parametric Wilcoxon Paired Signed Rank test (WPSR) for RCP4.5 to test for significant differences between the distributions of ensembles of the indices at 1.0°C, 1.5°C and 2.0°C. For RCP8.5 we followed the same procedure, but included the higher warming levels of 2.5°C and 3.0°C. We used the non-parametric Wilcoxon Sum Rank test (WSR) to test for significant differences between the distributions of the RCP4.5 and RCP8.5 ensembles of the indices at 1.0°C, 1.5°C and 2.0°C. We presented the results of the WPSR and the WSR as matrix/heat maps (see Figure 4 for example). To determine whether the models agreed on the direction of change, we set a criterion that at least 75% of the members needed to be in agreement (Sillmann *et al.,* 2013b; Pinto *et al.,* 2016).

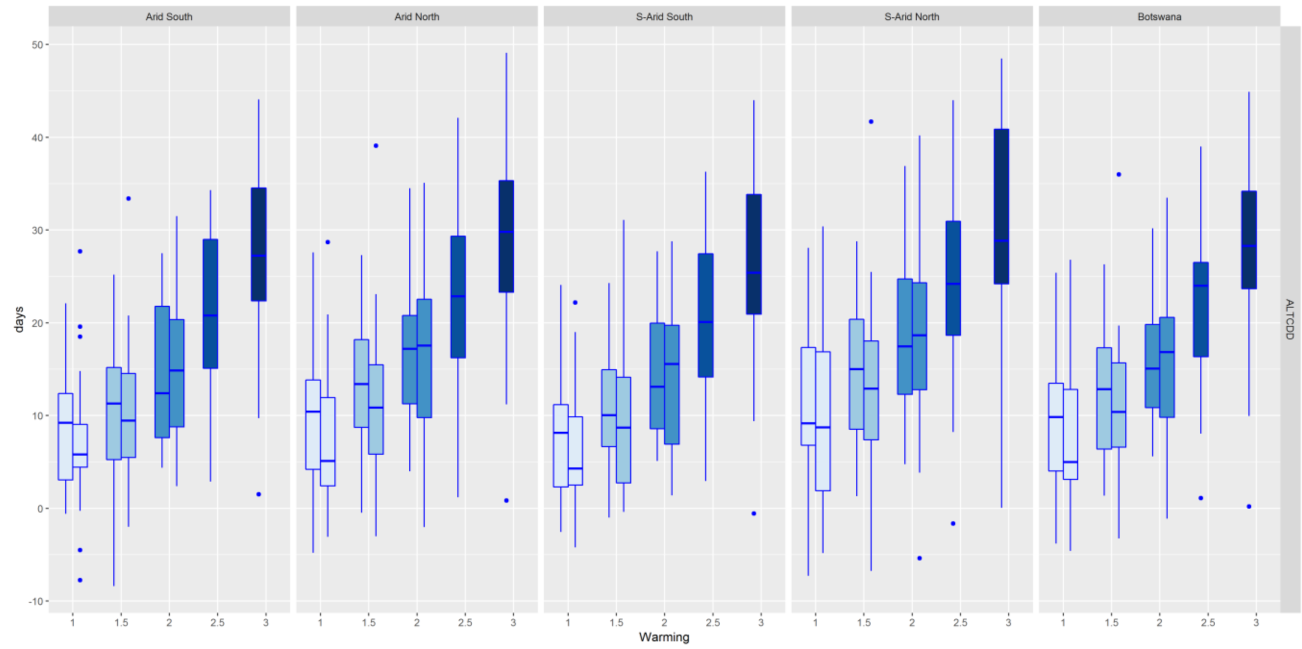

Figure 3: Example (for Botswana) of the box and whisker plots we used to show the changes in extreme precipitation indices (ALTCDD) across an ensemble of 20 and 24 participating model members for RCP4.5 and RCP8.5 respectively. The changes are at 1.0°C, 1.5°C and 2.0°C above pre-industrial levels for RCP4.5 and RCP8.5, as well as at 2.5°C and 3.0°C for RCP8.5.

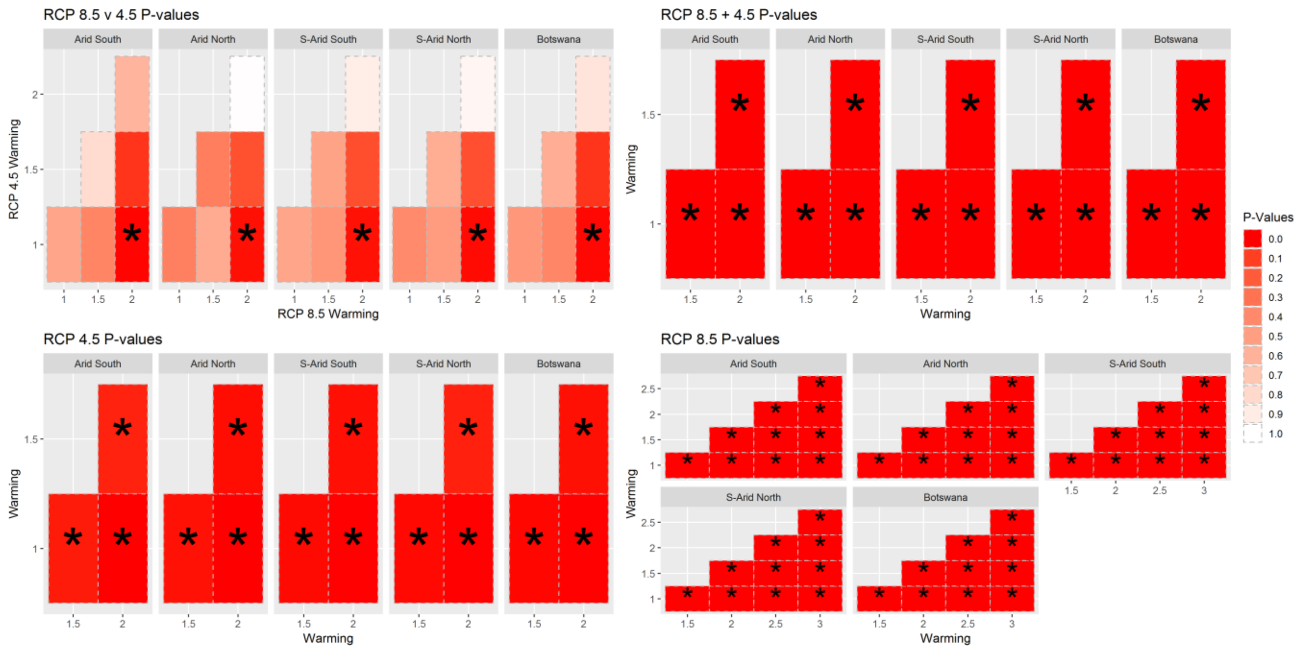

Figure 4: Example (for Botswana) of the heat maps we produced using the WPSR test results. The maps above show: significant differences between the 24 member ensemble spread of RCP8.5 and the 20 member ensemble spread of RCP4.5 (top left); the combined 44 member ensemble spread of RCP8.5 and RCP4.5 (top right); the 20 member ensemble spread of RCP4.5 for global warming levels of 1.0°C, 1.5°C and 2.0°C (bottom left); and the 24 member ensemble spread of RCP8.5 for global warming levels of 1.0°C, 1.5°C, 2.0°C, 2.5°C and 3.0°C (bottom right). * indicates statistical significance at the 95% confidence level.

d) Determining local impacts

Once we had examined projections for local climate changes at 1.5°C and higher global warming, we conducted an extensive literature review to determine the significance of these changes for each of the countries' vulnerable sectors, and to draw links with existing work. We identified key vulnerabilities based on an examination of the intended nationally determined contributions (INDCs), national adaptation plans (NAPs), climate change strategies, and related adaptation reports and policies. Country contexts were informed by country climate-change profiles developed for the African Development Bank (unpubl.) and the ND Gain index. Once we had identified the vulnerable sectors, we explored the possible impacts on these sectors using two types of studies: (i) studies that examined impacts at different time scales and different emission scenarios; (ii) studies that assessed the impacts at different temperature increments. We prioritised studies that assessed impacts at local and regional scales, and used global studies only as a last resort. Where applicable, we supplemented the information using Climate Analytics' Local SLR and RegioCrop tools for sea-level rise and crop yields.

In order to link time scales and emissions scenarios to the relevant temperature intervals, we used either the SRES (Special Report on Emissions Scenarios) or RCP emissions scenarios. The SRES scenarios were used for the 3rd and 4th IPCC assessment reports, and by many valuable studies, and represent emission trajectories on different development pathways. These include high development trajectories with economic growth (A1 and A2 scenarios) and environmental growth (B1 and B2 scenarios). The RCP scenarios were adopted for the IPCC's 5th assessment report and represent low (RCP4.4), medium (RCP6) and high (RCP8.5) emission pathways (Rogelj *et al.,* 2012). The global mean temperature increases above pre-industrial levels under each of the SRES and RCP scenarios were based on median projections for 2100, following Rogelj *et al.* (2012). We followed Arnell *et al.* (2004) for mean temperature increases in the 2020s, 2050s and 2080s.

Using R software, we linked results from past studies to global temperature increases at relevant emission scenarios in order to produce a linear regression model for the impacts at 1.5°C, 2°C, 2.5°C, and 3°C. The linear regression allowed us to quantify impacts of each increment of warming by creating a statistical range of possible impacts at each of these intervals. While the linear regression allowed us to quantify the estimated impacts of 1.5°C, these estimates assumed no thresholds being exceeded, and did not take any feedback loops or adaptation actions into account. Therefore, these estimates do not represent actual values of change, but rather indicate the possible repercussions incurred if immediate adaptation action is not taken. Determining the exact impact of warming temperatures on different sectors is complex; however, our analyses enabled us to estimate the potential sector losses and gains experienced by each country. We describe our findings in country-specific infographics and information briefs, which are available on the ASSAR website.

3. References

African Development Bank. 2018. National Climate Change Profiles (Namibia, Kenya, Ethiopia, Mali and Ghana) for the Climate Change and Green Growth Division of the African Development Bank: Unpublished.

Amekudzi, L., Yamba, E., Preko, K., Asare, E., Aryee, J., Baidu, M. and Codjoe, S. 2015. Variabilities in rainfall onset, cessation and length of rainy season for the various agro-ecological zones of Ghana. *Climate*, 3(2), 416–434.

Arnell, N.W., Livermore, M.J., Kovats, S., Levy, P.E., Nicholls, R., Parry, M.L. and Gaffin, S.R. 2004. Climate and socio-economic scenarios for global-scale climate change impacts assessments: characterising the SRES storylines. Global Environmental Change, 14(1), 3-20.

Dai, A. 2006. Precipitation characteristics in eighteen coupled climate models. *Journal of Climate,* 19(18), 4605–4630.

Food Agriculture Organization. 2006. WRI Major Watersheds of the World Delineation Database. [Website] Accessed: 3 September 2018.

Henley, B.J., and King, A.D. 2017. Trajectories toward the 1.5°C Paris target: Modulation by the Interdecadal Pacific Oscillation. *Geophysical Research Letters*, 44(9), 4256-4262.

Hijmans, R.J., Cameron, S.E., Parra, J.L., Jones, P.G. and Jarvis, A. 2005. Very high resolution interpolated climate surfaces for global land areas. *International Journal of Climatology*, 25(15), 1965–1978.

Intergovernmental Panel on Climate Change. (2014). Long-term Climate Change: Projections, Commitments and Irreversibility. In *Climate Change 2013 – The Physical Science Basis: Working Group I Contribution to the Fifth Assessment Report of the Intergovernmental Panel on Climate Change*, 1029-1136. Cambridge: Cambridge University Press.

Intergovernmental Panel on Climate Change. (2018). Global Warming of 1.5 °C: an IPCC special report on the impacts of global warming of 1.5 °C above pre-industrial levels and related global greenhouse gas emission pathways, in the context of strengthening the global response to the threat of climate change, sustainable development, and efforts to eradicate poverty. Cambridge: Cambridge University Press.

Kharin, V. V., Zwiers, F.W., Zhang, X. and Wehner, M. 2013. Changes in temperature and precipitation extremes in the CMIP5 ensemble. *Climatic Change,* 119(2), 345–357.

Klein Tank, A.M.G., Zwiers, F.W. and Zhang, X. 2009. *Guidelines on Analysis of extremes in a changing climate in support of informed decisions for adaptation*. Geneva, Switzerland.

Moses, O. 2017. Heat wave characteristics in the context of climate change over the past 50 years in Botswana. *Botswana Notes and Records*, 49(0), 13–25.

Nkemelang, T., New, M. and Zaroug, M. 2018. Temperature and precipitation extremes under current, 1.5 °C and 2.0 °C global warming above pre-industrial levels over Botswana, and implications for climate change vulnerability. *Environmental Research Letters,* 13(6.

O'Gorman, P.A. 2015. Precipitation Extremes Under Climate Change. *Current Climate Change Reports*, 1(2), 49–59.

Pinto, I., Lennard, C., Tadross, M., Hewitson, B., Dosio, A., Nikulin, G., Panitz, H.J. and Shongwe, M.E. 2016. Evaluation and projections of extreme precipitation over southern Africa from two CORDEX models. *Climatic Change,* 135(3–4), 655–668.

R Core Team. 2018. R: A language and environment for statistical computing. R Foundation for Statistical Computing, Vienna, Austria. Available: https://www.R-project.org/.

Rogelj, J., Meinshausen, M. and Knutti, R. 2012. Global warming under old and new scenarios using IPCC climate sensitivity range estimates. *Nature Climate Change*, 2(4), 248-253.

Sillmann, J., Kharin, V. V., Zhang, X., Zwiers, F.W. and Bronaugh, D. 2013a. Climate extremes indices in the CMIP5 multimodel ensemble: Part 1. Model evaluation in the present climate. *Journal of Geophysical Research Atmospheres*, 118(4), 1716–1733.

Sillmann, J., Kharin, V. V., Zwiers, F.W., Zhang, X. and Bronaugh, D. 2013b. Climate extremes indices in the CMIP5 multimodel ensemble: Part 2. Future climate projections. *Journal of Geophysical Research Atmospheres*, 118(6), 2473–2493.

Taylor, K.E., Stouffer, R.J. and Meehl, G.A. 2012. An overview of CMIP5 and the experiment design. *Bulletin of the American Meteorological Society*, 93(4), 485–498.

Trabucco, A. and Zomer, R. (in press). Global Aridity Index (Global-Aridity) and Global Potential Evapo-Transpiration (Global-PET) Geospatial Database. *CGIAR Consortium for Spatial Information*.

Trouet, V. and Van Oldenborgh, G.J. 2013. KNMI Climate Explorer: A Web-Based Research Tool for High-Resolution Paleoclimatology. *Tree-Ring Research*, 69(1), 3–13.

Westra, S., Fowler, H.J., Evans, J.P., Alexander, L. V., Berg, P., Johnson, F., Kendon, E.J., Lenderink, G., *Roberts, N.M.* 2014. Future changes to the intensity and frequency of short-duration extreme rainfall. *Reviews of Geophysics*, 52(3), 522–555.